Proceedings World Geothermal Congress 2026
Calgary, Canada, June 8 – 11, 2026

Beyond Gringarten: A closed-form solution to predict the temperature evolution of geothermal doublets (in porous, low-enthalpy settings)

C. Wallmeier[1], P. J. Vardon[1] and A. Daniilidis[1]
[1] Delft University of Technology
a.daniilidis@tudelft.nl

Keywords: Direct-Use, Lifetime, Analytical, Production Temperature

1 INTRODUCTION

Deep geothermal projects are often characterized by high investment costs and low operational costs. This means that they are economically viable - and increasingly competitive to other sources of energy - if their lifetime is long enough (Daniilidis et al. 2017). Lifetime is generally considered to depend on the temperature of the produced water, as it controls the amount of energy that can be extracted and sold (Daniilidis et al. 2017).

In typical doublet systems, the re-injected cold water eventually reaches the producer well and causes production temperature to decline. The onset of this decline is known as thermal breakthrough. An equation to calculate time of breakthrough (based on the thermal conductivity, thickness and porosity of a homogeneous reservoir, and the spacing and flowrate of the wells) was first published 50 years ago (Gringarten and Sauty 1975). But while breakthrough is frequently equated with usable lifetime (Limberger et al. 2018, Fan et al. 2022), this is a very pessimistic approach since the minimum acceptable output temperature of a doublet may be substantially below its initial production temperature. The decay of temperature after breakthrough is complicated to predict (Sbai and Larabi 2023) because it is a process that combines multiple components of advection and conduction.

With sufficient knowledge about geological properties, geometry, and heterogeneity, reservoir cooling can be modelled numerically and the evolution of production temperature can be predicted. However, even in data-rich settings, significant uncertainties remain (Hamm et al., 2010). To address them, model ensembles are used to capture the impact of uncertainties in physical properties (Wang et al., 2023) or different realizations of heterogeneity (Budai et al., 2024, Chen et al., 2025). However, such models require significant time and specialist skills to set up and run.

Closed-form models ($T_{Prd}(t) = xxx$) that predict production temperature in a simpler and faster way are a valuable alternative. They can run almost instantly and do not depend on specific software. To our knowledge, there is no model that returns the full temperature evolution of the produced water and is robust, accurate, and fast for conduction-dominated low-enthalpy settings. In this study, we present such a model. It covers a wide range of geological and engineering parameters which are most relevant for the cooling behavior of a geothermal system and which can be estimated reasonably well when little subsurface information is available.

2 METHODS AND RESULTS

We used numerical models - including an accurate physical description of the subsurface processes and properties - to calibrate an equation that predicts the evolution of production temperature accurately across the parameter range.

The final closed-form equation is:

$$T_{prd}(t) = T_{Inj} + \Delta T * \frac{1}{log_{10}\left(10 + c(a^t\text{-}1)\right)^m} \quad (1)$$

where *a*, *c* and *m* are coefficients that can be calculated directly from known doublet parameters. The derivation of the coefficients is described in the following steps.

2.1 Step 1: Numerical reference simulations

We simulated an ensemble of 600 doublets in homogeneous reservoirs numerically and output their production temperature over 100 years. The models differ in their combination of seven parameters that govern the cooling behavior of a doublet (Tab. 1a): Reservoir height *H*, reservoir depth *D*, porosity φ, temperature gradient T_{Grad}, Well spacing *L*, flow rate *Q*, and extracted temperature *dT*. They were distributed in a

uniform, semi-random way, targeting breakthrough times between 10 - 50 years and covering the parameter space thoroughly, while omitting unrealistic combinations such as cooling systems.

We fixed parameters that have been shown - previously or in test simulations - to not significantly impact the shape of the production temperature curve (Tab. 1b). A third group of parameters can be derived from the ones described above. For example, initial reservoir temperature follows from depth and thermal gradient. In order to find the simplest and most concise expression for $T_{Prd}(t)$, we investigated a number of such derived and alternative descriptions. The final choice of relevant derived parameters is listed in Tab. 1c.

Table 1.

Variable	Description	Unit	Min	Max
1a)				
H	Reservoir thickness	m	20	160
D	Reservoir depth	m	1000	3500
T_{Grad}	Temperature gradient	K/m	0.025	0.035
φ	porosity	-	0.15	0.25
L	Well spacing	m	400	1600
Q	Flow rate	m^3/s	150	450
dT	Extracted temperature	K	10	100
1b)				
	Surface temperature	°C	10	
	Th. cap. reservoir (dry)	$J/(m^3K)$	2300	
	Th. cap. Confining (dry)	$J/(m^3K)$	2300	
	Th. cond. reservoir	W/(mK)	3	
	Th. cond. confining	W/(mK)	2	
	Permeability	mD	Function of φ (Willems et al., 2020)	
1c)				
T_0	Initial reservoir temp.	°C	$T_{Surf} + D * T_{Grad}$	
T_{Inj}	Injection temp.	°C	$T_0 – dT$	
μ_{Rel}	Relative viscosity contrast	-	μ_{Inj} / μ_{Prd} (Spivey and North, 2004)	
t_{Grin}	Calculated time of breakthrough	Years	Gringarten and Sauty, 1975	

We ran the simulations using the finite volume simulator open-DARTS (Voskov et al., 2024). In the center of the model near the doublet, mesh resolution was 10m horizontally and 2m vertically. T_{Prd} was observed at reservoir depth and at time steps of 0.5 years.

2.2 Step 2: Equation Form

The general equation form for any doublet setup has to meet three conditions: 1) It has to begin with a plateau at initial reservoir temperature T_0. 2) It has to end asymptotically in a second plateau at T_{Inj}. 3) In the middle part, it has to follow an inverted S-shape. Conditions 1 and 2 are met by setting:

$$T_{Prd(t)} = T_{Inj} + \Delta T * S(t) \tag{2}$$

where S(t) starts at 1 and drops towards 0. Condition 3 is met by setting

$$S(t) = \frac{1}{log_{10}\left(10 + c(a^t\text{-}1)\right)^m} \tag{3}$$

This equation can be described as a modified, asymmetric logistic function (Fig. 1). The combination of the three coefficients {*a*, *c*, *m*} allows the curve shape to be tailored accurately to match time of breakthrough, initial cooling behavior, and asymptotic flattening of any doublet scenario.

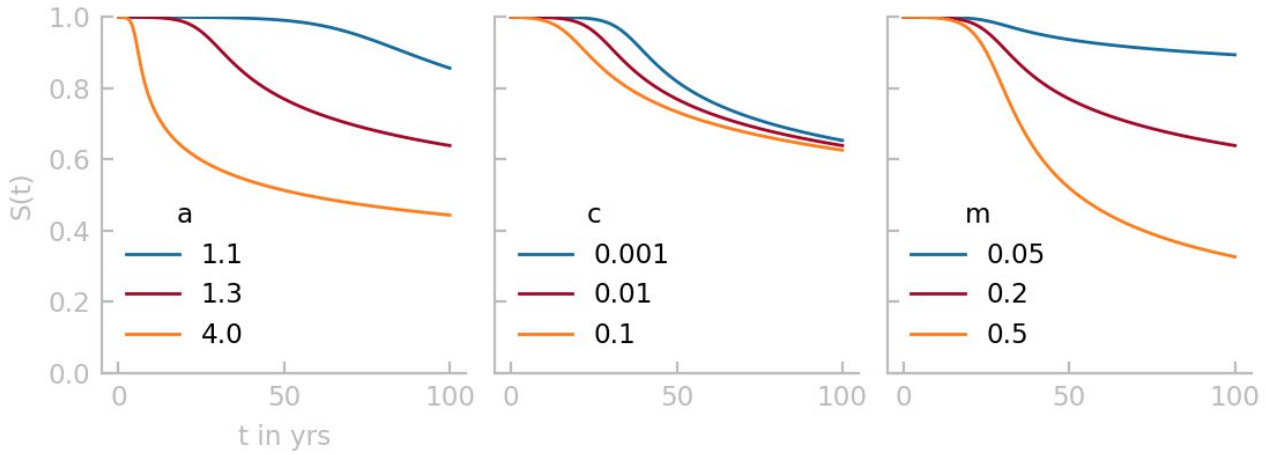


Fig. 1 Influence of each coefficient on the shape of S(t). Both *a* and *c* control breakthrough and initial steepness, but in different combinations. *m* controls the extent of the drop and onset of curve flattening.

2.3 Step 3: Fitting coefficients

Using curve fitting, we identified the best set of {*a*, *c*, *m*} for each training curve. We calculated the root-mean squared error (RMSE) between each observed curve and its fit. A small RMSE confirms that at any point in time, T_{Prd} is described with high accuracy. However, for the purpose of predicting the lifetime of a system, the error in the *x*-direction is just as important. Therefore, we investigated the horizontal mismatch in the part of the curve with the steepest drop, where discrepancies are most likely and most relevant. We calculated the mean average error (MAE) for when each full degree is reached, for the time from thermal breakthrough until a drop of 10 degrees was reached or for 20 years (whichever occurred first).

2.4 Step 4: Assigning doublet parameters to coefficients

Next, we mapped the fitted coefficients {*a*, *c, m}* to the selected doublet parameters (Tab. 1). Sensitivity analysis and scatter plot inspection were used to identify the parameters that each coefficient depends on. They are for both *a* and *c*: {μ_{Rel}, t_{Grin}, *H}* and for *m*: {*L, Q}.*

Standard and symbolic regressions were used to determine the form of each equation, and a subsampling bootstrapping algorithm revealed the best-fitting numeric coefficients. The equations for *a, c* and *m* are:

$$a = 1.044 + \frac{8.903}{\mu_{rel}\, t_{Grin} + \frac{882.6}{H} - 12.02} \tag{4}$$

$$log_{10}(c) = \frac{1}{0.35 + \mu_{rel}} \left(\frac{80.35}{t_{Grin} + \frac{H}{t_{Grin}}} - 7.642 \right) \tag{5}$$

$$m = 0.2966 - \mathrm{L}\left(\frac{0.0138}{Q} + 0.000094\right) \tag{6}$$

2.5 Step 5: Verification

We verified the final T_{Prd}-equation on a set of 100 test cases. These were generated in the same way as the training cases, but not involved in steps 2-4. For each test case, we calculated first {*a*, *c*, *m*} according to eq. 4-6 and then T(t).

Fig. 2a shows the predicted temperature curves for a random subset of 10 test cases compared with their numerical simulations. The fit is close throughout. This is also represented by the errors across all 100 test cases (Fig. 2b): The average vertical error is 0.2K, and 97 cases have an error below 1K. The three remaining cases are below 2K. Horizontally, the average error is one year. Some outliers exist, two of which are mispredicted by more than five years. However, closer inspection reveals that these are cases with a very flat temperature profile, meaning the error is of less practical importance because temperature is very stable throughout the prediction period.

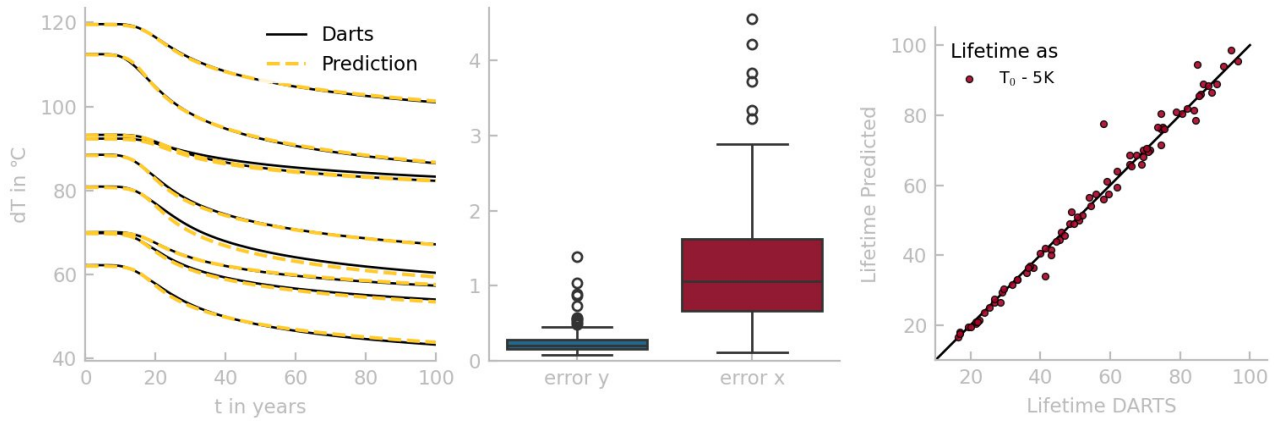


Fig. 2. A) Predicted versus numerically simulated temperature profiles for test cases. (for plot compactness, y-axis displays dT, i. e. dT=0 corresponds to T_{Inj}. B) Vertical RMSE (T in K) and horizontal MAE (t in years) for the 100 test cases. C) Predicted vs. numerically observed lifetimes.

As a more practical test, we predicted system lifetime for each case and compared it with the lifetimes observed in the open-DARTS simulations. We defined lifetime as the moment when $T_{Prd} = T_0 - 5K$. This succeeds (Fig. 2c) with an RMSE below 3 years. Cases that did not reach a lifetime criterion within the 100 years of DARTS simulation could not be considered in this test.

3 CONCLUSION

A closed-form equation is proposed for the full production temperature evolution for low-enthalpy geothermal doublets. Coefficients of the equation have been calculated based on doublet parameters, i.e. depth, thickness and porosity of the targeted reservoir, the expected thermal gradient, well spacing, flow rate and injection temperature. This means that the production temperature of geothermal doublets can be predicted without the use of numerical models. The equation covers a large parameter space that is relevant to low-enthalpy, conduction-dominated geothermal systems continuously without gaps or jumps. It facilitates extensive ensembles to be evaluated as it runs near-instantly and it can be implemented in any programming language or spreadsheet editor and can therefore easily be combined with prior or subsequent analyses.

REFERENCES

Budai, S., Willems, C.J.L., Colombera, L., Westaway, R.: Influence of sedimentary architecture on static connectivity and geothermal doublet performance (Mezőberény, SE Hungary). *Marine and Petroleum Geology,* **164**, (2024), 106820

Chen, Y., Rongier, G., Voskov, D., Daniilidis, A.: Robust Framework to Evaluate Representative Heterogeneity for the Simulation of Direct-Use Geothermal Systems, *Proceedings*, SPE Reservoir Simulation Conference, Galveston, US (2025)

Cranmer, M.: Interpretable Machine Learning for Science with PySE and SymbolicRegression.jl, *Princeton University and Flatiron Institute,* (2023)

Daniilidis, A., Alpsoy, B., Herber, R.: Impact of technical and economic uncertainties on the economic performance of a deep geothermal heat system. *Renewable Energy* **114** (2017), 805–816.

Fan, Y., Zhang, S., Huang, Y., Pang, Z., Li, H.: Determining the Recoverable Geothermal Resources Using a Numerical Thermo-Hydraulic Coupled Modeling in Geothermal Reservoirs. *Front. Earth Sci.* **9** (2022)

Gringarten, A.C., Sauty, J.P.: A theoretical study of heat extraction from aquifers with uniform regional flow. *Journal of Geophysical Research* (1896-1977) **80**, (1975) 4956–4962.

Hamm, V., Castillo, C., Le Brun, M., Goyeneche, O.: Mise en œuvre de la gestion de la ressource géothermique du Dogger de la région Ile-de-France dans le cadre du dispositif d'acquisition et de stockage des données, *BRGM/RP-58834-FR*, (2010)

Limberger, J., Boxem, T., Pluymaekers, M., Bruhn, D., Manzella, A., Calcagno, P., Beekman, F., Cloetingh, S., van Wees, J.-D.: Geothermal energy in deep aquifers: A global assessment of the resource base for direct heat utilization, *Renewable and Sustainable Energy Reviews* **82**, (2018), 961–975

Sbai, M.A., Larabi, A.: Analyzing the relationship between doublet lifetime and thermal breakthrough at the Dogger geothermal exploitation site in the Paris basin using a coupled mixed-hybrid finite element model. Geothermics, 114 (2023)

Spivey, J.P., North, R.: Estimating Density, Formation Volume Factor, Compressibility, Methane Solubility, and Viscosity for Oilfield Brines at Temperatures From 0 to 275 ° C, Pressures to 200 MPa, and Salinities to 5.7 mole/kg, *Journal of Canadian Petroleum Technology*, **43,** (2004)

Voskov, D., Saifullin, I., Novikov, A., Wapperom, M., Orozco, L., Seabra, G.S., Chen, Y., Khait, M., Lyu, X., Tian, X., Hoop, S. de, Palha, A.: open Delft Advanced Research Terra Simulator (open-DARTS). *Journal of Open Source Software,* **9**, (2024), 6737

Wang, Y., Voskov, D., Daniilidis, A., Khait, M., Saeid, S., Bruhn, D.: Uncertainty quantification in a heterogeneous fluvial sandstone reservoir using GPU-based Monte Carlo simulation. *Geothermics,* **114**, (2023), 102773

Willems, C.J.L., Vondrak, A., Mijnlieff, H.F., Donselaar, M.E., Kempen, B.M.M. van: Geology of the Upper Jurassic to Lower Cretaceous geothermal aquifers in the West Netherlands Basin -an overview, *Netherlands Journal of Geosciences*, **99**, (2020)